URBAN CHANGE EXTRACTION FROM HIGH RESOLUTION SATELLITE IMAGE

M. S. Moeller [a, *], T. Blaschke [b]

[a] GIOS, ASU, Global Institute of Sustainability, Arizona State University, Tempe, AZ 85287-3211
matthias.moeller@asu.edu
[b] Z_GIS, Center for Geoinformatics, Paris-Lodron-Universität Salzburg, Schillerstrasse 30, 5520 Salzburg, Austria,
thomas.blaschke@sbg.ac.at

Commission II

KEY WORDS: change detection, large scale urban monitoring, urban growth, PCA, NDVI, IHS, Quickbird.

ABSTRACT:

Very high resolution space borne imagery is essential for a large scale and very detailed urban monitoring and the Quickbird sensor is one of those. It offers images with a spatial resolution of 0.61 m (panchromatic) and 2.44 m (four multispectral bands). Not only a mapping and cadastral surveying of urban objects can be done based on that kind of imagery. A special task is the detection of changed urban objects such as buildings and altered surface materials. This paper compares three different indices for their usability of detecting changes and finally presents a mixture of indices working best for the differentiation of man made urban objects.

KURZFASSUNG:

Sehr hoch auflösende Satellitenbilder sind notwendig für ein großmaßstäbiges und sehr detailliertes Monitoring städtischer Gebiete. Der Quickbird Sensor liefert dafür geeignete Aufnahmen mit einer räumlichen Auflösung von 0.61 m (panchromatisch) und 2.44 m (vier multispektrale Kanäle). Diese Bilddaten können nicht nur für das eigentliche Kartieren von urbanen Objekten verwendet werden, sondern sie eignen sich auch für die Analyse von Änderungen einzelner Objekte. In diesem Beitrag werden drei verschiedene Indizes daraufhin getestet, welcher sich zur Differenzierung von veränderten Objekten am besten eignet.

1. INTRODUCTION

Urban areas are those regions on earth for which the most dynamic changes can be observed. They are characterized by a trend of permanent expansion and growth. Meanwhile and for the first time ever more than 50 % of earth' entire human population can be found in urban areas and the trend is going on. Remote sensing can be performed on several levels of resolution or levels of detail, e.g. it is scale dependent. Conceptually, scale corresponds to a 'window of perception'. More practically, scale represents a measuring tool composed of two distinct components: grain and extent. Grain refers to the smallest intervals in an observation set, while extent refers to the range over which observations at a particular grain are made (O'Neill and King, 1998). From a remote sensing perspective, grain is equivalent to the spatial, spectral, and temporal resolution of the pixels composing an image, while extent represents the total area, combined bandwidths and temporal duration covered within the scene (Hay et al., 2001).

In many day-to-day applications scale is more or less used synonymously with the spatial resolution of the analyzed imagery as a clearly measurable dimension. The pixel size of optically remotely sensed imagery ranges from 0.05 m - 1000 m (Neer 1999). But a refined spatial resolution shows a strong trend of negative correlation with the image repeat cycle (when a second image of the same area may be acquired) and a positive correlation with the related data costs. In practice one has to find a compromise between a high spatial resolution and the time span between two data sets needed to be purchased in order to monitor changes cost-effectively. In a recent example for the Phoenix metropolitan area Moeller (2004) uses remote sensing imagery at a medium scale level ranging from 1:75.000 to 1:100.000 although finer resolutions were available at least for several points in time. This analysis led to reasonable results in terms of urban growth for the Phoenix metropolitan area. These time series outlines the ongoing development on a grid cell level of 0.25 km². A clear differentiation between several stages of expansion in terms of growth direction and growth distance measured from the city center has been performed based on these image series (Moeller 2004). This research was conducted for three major land use land cover classes typical for this region: urban, farmland, natural land. For more detailed urban remote sensing applications scales typically range from 1:500 - 1:25.000. The larger scales has been proofed for detailed surveying tasks e.g. for cadastral mapping on a building level. Those images are mainly acquired by aerial cameras with analog and newly developed digital sensors (Moeller 2003). But this kind of imagery is still expensive. Therefore, the empirical study described in this paper is based on high resolution satellite imagery. The '1m-resolution' sensor generation including Quickbird and Ikonos is today regarded as being most useful for an urban monitoring (Banzhaf and Netzband 2004). We investigate this potential as well as the limits in terms of detect ability of objects for a rapidly changing sub-urban area north of Phoenix and compare several change detection indices.

* Corresponding author.

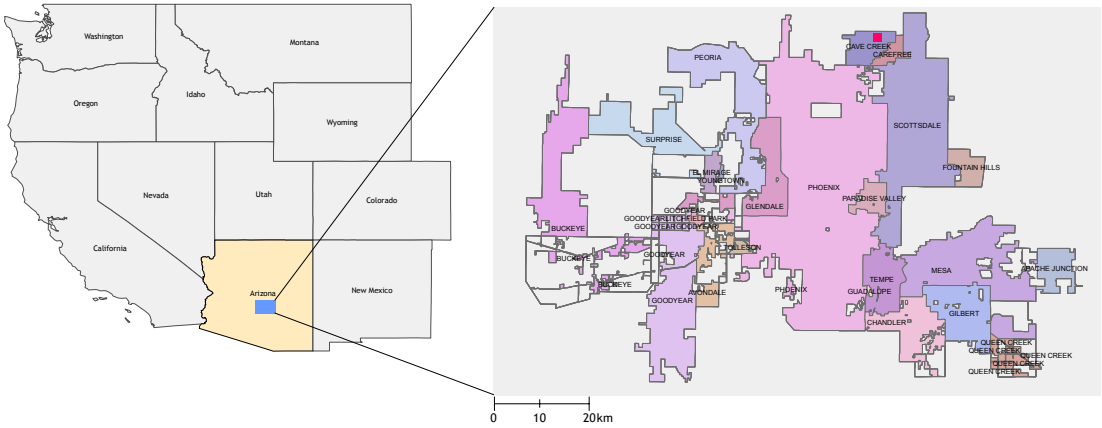

red rectangle indicates the location of the Cave Creek area

Figure 1. Location of the Phoenix metropolitan area

2. CHANGES IN THE PHOENIX METROPOLITAN AREA

The Phoenix metropolitan area (fig. 1) is one out of three regions in the U.S. with the strongest economic growth. During the last 30 years the size of the PHX metro area has nearly doubled and population has tripled during this period. Enough open space for future growth is available for development and an end of the expansion is still not in sight. For Phoenix, the only limiting factor for this growth is the accessibility of fresh water (Greater Phoenix 2100, 2003).

3. TEST SITE AND DATA SETS

The test site used in this research is located north of Phoenix and belongs to the Cave Creek area. Cave Creek is one of the newly developed regions. Large amount of natural and undisturbed land (e.g. parts of the Sonoran desert) is still available at comparably low costs. As a consequence new construction zones tend to include relatively large buildings on large parcels. Figure 2 shows a 500m x 500m subset of such a newly build up area which is part of the test site. Typical for the city of Cave Creek, a relatively large construction, and newly established buildings can be clearly detected by the observer's eye. The study area has been recorded twice by the Quickbird sensor covering a two year period (2. Jan. 2003; 12. Jan. 2005).

Both data sets have been acquired in panchromatic and in multispectral mode. The Quickbird standard imagery came as a pan-sharpened visible/infrared data set with a 0.7 m spatial resolution pre-processed to this level by Digital Globe 2005. The radiometric resolution is 16 bit (in fact 11 bit, but during the preprocessing those data have been up-sampled to 16 bit). Pan-sharpening techniques use the high resolution panchromatic information and fuse the four band multi spectral information with the pan band. We use a procedure which also includes a motion correction of the displaced imagery caused by spacecraft motion during data acquisition. The pan-sharpening method originally uses the UNB algorithm developed by the University of New Brunswick by Zhang 2002 (a,b) for Ikonos and Landsat Thematic Mapper imagery.

The Quickbird standard imagery does provide a geometric accuracy of up to 14-meter RMSE (up to 23-meter CE 90 %). With the underlying USGS 10 m DEM both imagery have been orthorectified with a much higher spatial accuracy. This guarantees a high spatial confidence for both imagery one to each other. An atmospheric correction has been applied to both imagery eliminating disturbances caused by different atmospheric condition during image acquisition. Finally, a 716 x 716 pixel subset has been cut from the original images.

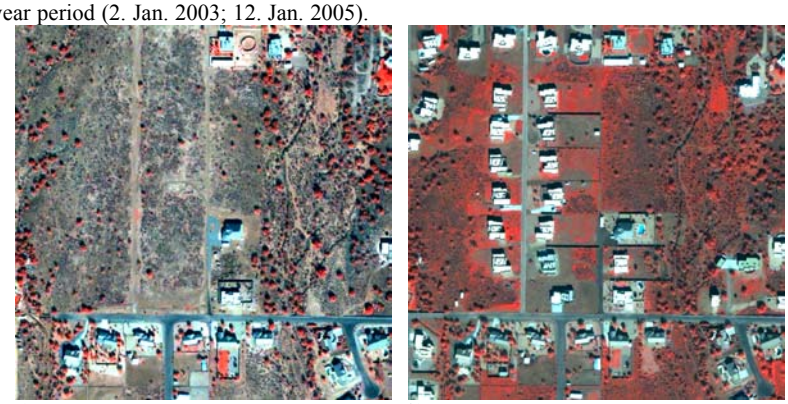

a) CIR 2003
R=IR, G=red, B=green, size 501m x 501m

b) CIR 2005

Figure 2. Quickbird color infrared pan-sharpened images of the study site

4. CHANGE DETECTION

4.1 Change detection analysis and object extraction

This paper presents a comparative study of several image indices: Normalized Differenced Vegetation Index (NDVI), Principle Component Analysis (PCA), Intensity, Hue and Saturation (IHS). These three indices have been applied to the high resolution Quickbird imagery following the approach of mathematical functions (1). These indices are tested in this paper for their suitability for the detection of urban feature changes.

The automated detection of changes especially in urban areas started in the early 1980s. Howarth and Boasson (1983) tested the Principal Component Analysis (PCA) and vegetation indices for a change detection of urban features by using Landsat Multispectral Scanner (MSS) imagery in a low resolution scale level. Li and Yeh (1998) have performed a PCA change detection classification based on a medium scale level by the use of Landsat Thematic Mapper TM imagery for the growth of Pearl River Delta region, China. Meanwhile, there are literally hundreds of change detection applications using the Landsat/Aster type of resolution (15-30 m) (Lu et al. 2003).

Since the advent of the Ikonos-2 sensor in 1999 satellite born imagery at high spatial resolution (1 to 4 m) is commercially available. After the successful launch of Quickbird in 2001 prices went down and a mass market emerged. Still, more and more studies and scientific papers claim that the need for new classification approaches increases (e.g. Blaschke and Strobl, 2001; Blaschke et al. 2004; Benz et al. 2004). Many authors suggest object based analysis for such kind of imagery and use various kinds of image segmentations as an initial step to derive groups of pixels. The principal idea has already been introduced in literature by Kettig and Landgrebe (1976). A number of indices have been proofed reliable for a change detection analysis in combination with an object based image analysis approach (O'Hara 2005). A water index has been calculated in this study, the NDVI and the IHS components have been established too for time 1 (T1) and time 2 (T2). Finally, all indices were compared in terms of changes in an object based environment.

water index = [Blue + Green] / NIR (1)
r = Green, g = Red, b = NIR -> IHS (2)

The following tests use the NDVI and IHS as described by O Hara (2005) and additionally include a detailed analysis of the PCA.

4.2 NDVI analysis

The NDVI is calculated as a normalized ratio (ranging from -1 through 1) from the NIR and the red band and emphases apparent vegetation (Sabins 1996). The index is directly related to the amount of active photosynthesis represented in the NDVI image as higher and brighter values (fig. 3a,b). Changes between the two dates are visible in fig. 3c and appear in purple tones. A dark tone indicates no change of a pixel value. White spots show strong and healthy vegetation for both dates of data acquisition. The changes in fig. 3c do not appear clearly. The absolute values of change are relatively small and result in a hazy appearance. Changed features come up like shadows, and the contrast between new and old features is relatively low.

For a direct tracking of changed features such as individual buildings and surface material 44 and 18 geo-located reference points have been selected. Those reference points are superimposed in fig. 3a-c with symbols: circle for buildings, triangles for surfaces.

The reflectance changes for all reference points from 2003 and 2005 can be seen in a chart (fig. 3d-e). Actually the average value of a circle with a 2m diameter around each point has been considered. Blue lines and symbols indicate the NDVI values for 2003, 2005 NDVI values are represented by the orange lines and symbols. Objects 1-16 (fig. 3d) represent buildings without any physical changes (objects 17-44 have changed), object 9-18 (fig. 3e) show surfaces that did not change (surfaces 1-8 have been altered). Usually one would expect an identical value for unchanged objects. But comparing the first 16 points in 3e, differences are quite obvious for – certainly - unchanged objects. Especially object 5 shows a big difference. The same phenomenon can be observed in fig. 3e for objects 9-18. In fact objects 10 and 13 show a huge difference.

4.3 Hue index analysis

The hue component has been extracted from the transformed imagery. The IHS transformation is a widely used algorithm and mostly applied to imagery for pan-sharpening (Jensen 2004). Within the IHS transformation the original three band image is converted from the multi-spectral space into the color space with the following components: intensity (I), hue (H) and saturation (S).

Changed objects can be detected from the hue two-spectral composite in a magenta color in fig. 4c. Compared to the changes visible in the NDVI two-band-spectral composite (the 2003 and the 2005 hue component) the hue changes are more crisp and clear. Even the footprint of individual buildings can be easily outlined. White and bright values indicate no change for artificial (man made) objects and greenish tones show natural and unchanged surfaces.

When comparing the two hue charts (fig. 4e-d) with the NDVI charts (fig. 3e-d) there is an obvious differentiation for the hue index. Unchanged objects show more identical values in both charts, but some values are still mismatching (1, 5, 8, 10 for buildings and 9, 10, 11, 13, 15 for surfaces).

4.4 PCA analysis

PCA provides a method for the reduction of redundant information apparent in multi-dimensional databases. PCA represents any object with a much fewer information compared to the original image. Minimization of the correlation of multi-dimensional bands is performed by mathematically transforming the multi-band into another vector space with a new basis. (Li and Yeh 1998; Ricotta et al. 1999).

The change image composite (fig 5c) outlines the changes with the magenta color. Changes can be observed visually with a higher accuracy compared to the NDVI image (fig. 3c). Changes also appear crisper compared to the hue composite. Unchanged objects are represented with a light green to white color in fig. 5c. The value charts show a very high degree of congruence for unchanged objects in both categories buildings and surfaces. All unchanged objects consist of the same value in

2003 and 2005. On the other hand, changed objects can be differentiated with a high degree of reliability.

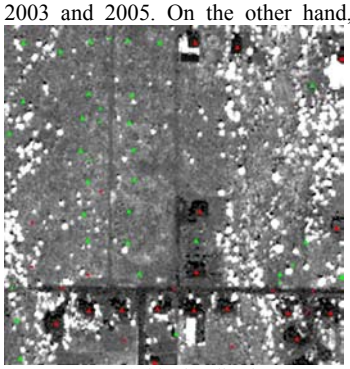

a) NDVI 2003 (8 bit visualization)

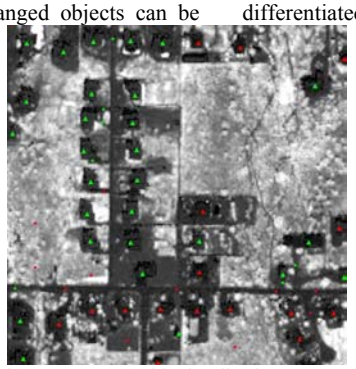

b) NDVI 2005 (8 bit visualization)

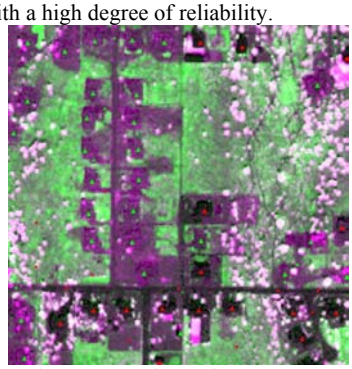

c) change composite (r,g,b:03,05,03)

triangle: building; circle: surface; green: change; red: no change

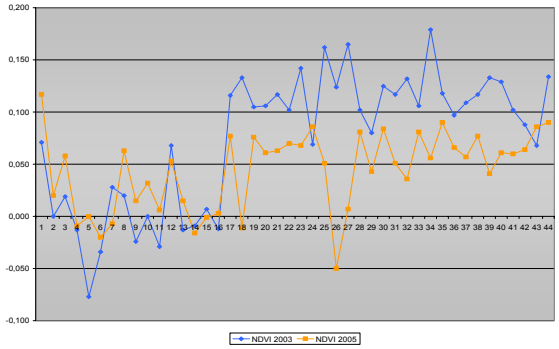

d) buildings

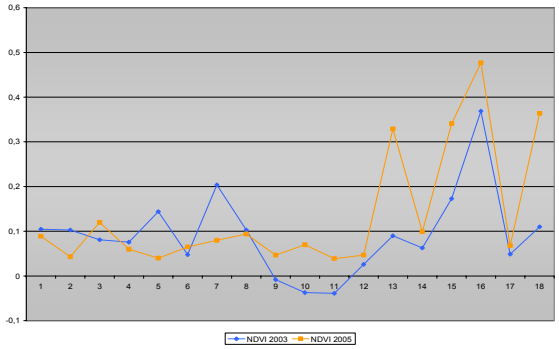

e) surfaces

Figure 3. NDVI images (2003 and 2005)

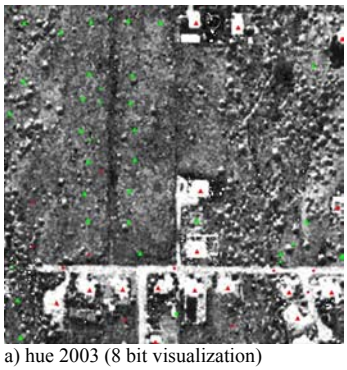

a) hue 2003 (8 bit visualization)

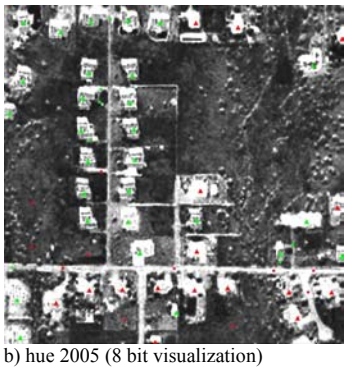

b) hue 2005 (8 bit visualization)

c) change composite (r,g,b:05,03,05)

triangle: building; circle: surface; green: change; red: no change

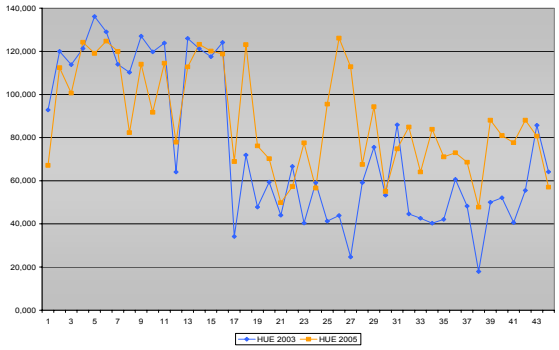

d) buildings

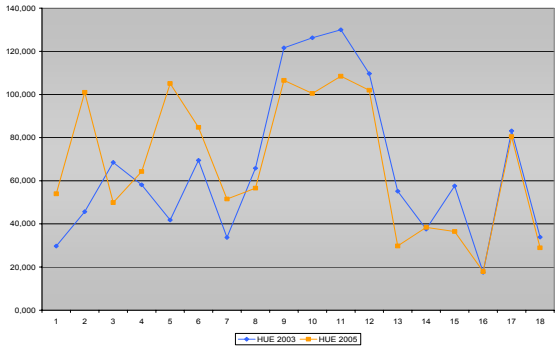

e) surfaces

Figure 4. Hue components (2003 and 2005)

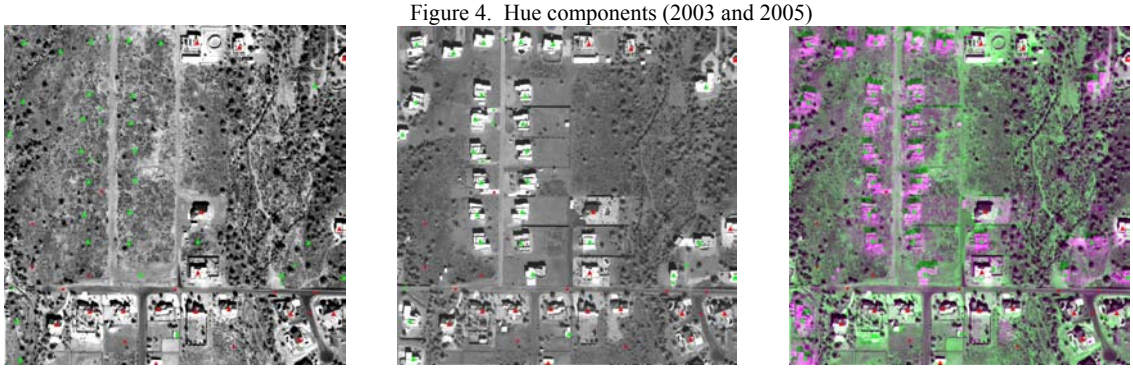

a) PCA 1 2003 (8 bit visualization) b) PCA 1 2005 (8 bit visualization) c) change composite (r,g,b:05,03,05)
triangle: building; circle: surface; green: change; red: no change

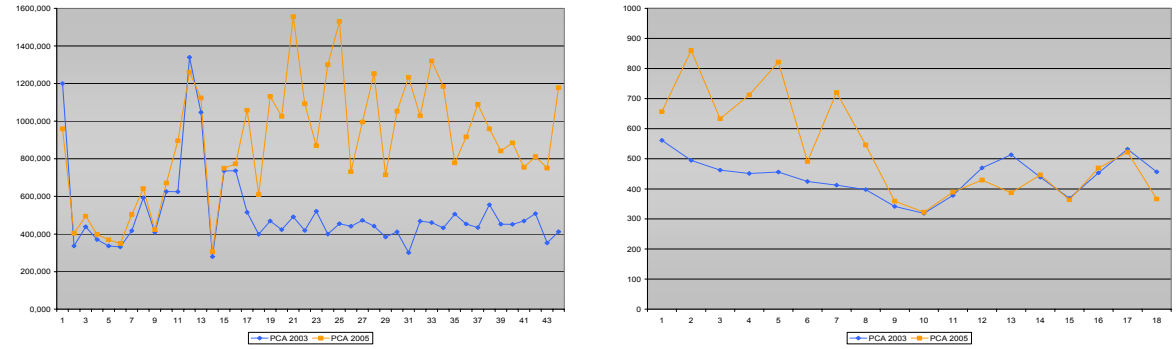

d) buildings e) surfaces

Figure 5. PCA first component (2003 and 2005)

5. COMPARISON OF THE RESULTS AND OUTLOOCK

Finally all values for the observed points (buildings and surfaces) have been analyzed for their significance representing a change or no change. For those points a correlation matrix has been computed and the resulting values are listed in table 1.

	building	surface	index
change	-0,351	-0,098	NDVI
no change	0,709	0,874	
change	0,045	-0,059	Hue
no change	0,754	0,971	
change	0,023	0,351	PCA
no change	0,953	0,735	

Table 1. Correlation of values changed and unchanged objects

The best differentiation of changed buildings can be observed for the newly introduced PCA index. The PCA also represents unchanged buildings with a high reliability. Unchanged surface materials are represented by the Hue index and changed surfaces can be differentiated by using the NDVI index.
Having these results in mind the next consequent step will be the implementation of the two date indices in an arbitrary environment. First tests with an object based approach led to promising results.

The analysis of changed urban objects such as buildings is not primarily necessary for metropolitan areas in developed countries. Especially so called informal settlements, mainly located in suburbs of metropolitan areas in less developed countries, will be investigated in the future. Special challenges for the detection of those objects are their diverse appearance in remotely sensed imagery. However, an automated procedure that allows the detection of changed urban objects could be from great interest in terms of urban security.

ACKNOWLEDGEMENTS

The National Science Foundation made this research possible under the grant of the AgTrans project. We thank Kumar Navulur, Digital Globe, USA and Markus Heynen, Definiens, Germany for their kindly support. We also thank Chris Eisinger for his intense support. He is the technical staff of Arizona State Universities Geological Department and provided us with Quickbird satellite data archived in the Urban Environmental Monitoring (UEM) project.

REFERENCES

Banzhaf, E., Netzband, M., 2004. Detecting urban brownfields by means of high resolution satellite imagery. In: *The International Archives of the Photogrammetry, Remote Sensing and Spatial Information Sciences*, XXXV, Part B, Comm. VII. pp. 460-466.

Digital Globe, 2005. QuickBird Imagery Products Product Guide. http://www.digitalglobe.com/downloads/QuickBird%20Imagery%20Products%20-%20Product%20Guide.pdf (accessed 31 Dec. 2005)

Greater Phoenix 2100, 2003. *Greater Phoenix regional atlas: A preview of the region's 50-year future, Greater Phoenix 2100*. Arizona State University, Tempe, AZ, USA.

Howarth, P., Boasson, E., 1983. Landsat digital enhancement for change detection in urban environment. *Remote Sensing of Environment*, 13, pp. 149-160.

Jensen, J., 2004. *Introductory Digital Image Processing*. Prentice Hall 3rd Edition.

Li, X., Yeh, A., G., O., 1998. Principal component analysis of stacked multi-temporal images for the monitoring of rapid urban expansion in the Pearl River Delta of Hong Kong, Pokfulam Road, Hong Kong. *Int. Journal of Remote Sensing*, 19 (8), pp. 1501 - 1518.

Lu, D., Mausel, P., Brondizio, E., Moran, E., 2003. Change detection techniques. *Int. Journal of Remote Sensing*, 25 (12), pp. 2365-2407.

Magsig, M. A., Dickens-Micozzi, M., Yuan M., 2002. Analysis of tornado damage on May 3rd, 1999 using remote sensing and GIS methods on high-resolution satellite imagery. *Weather Forecasting*, 17, pp. 382–398.

Möller, M., 2003. *Urbanes Umweltmonitoring mit digitalen Flugzeugscannerdaten.* Wichmann, Karlsruhe.

Möller, M., 2004: Monitoring Long Term Transition Processes of a Metropolitan Area with Remote Sensing. In: *Proceedings of the IGARSS 2004 Conference, Anchorage, AK,* on CD.

Möller, M., 2005. Remote Sensing for the Monitoring of Urban Growth Patterns. In: *The International Archives of the Photogrammetry, Remote Sensing and Spatial Information Sciences*, Vol. XXXVI - 8/W27, on CD.

Neer, J. T., 1999. High Resolution Imaging from Space - A Commercial Perspective on a Changing Landscape. In: *The International Archives of the Photogrammetry, Remote Sensing and Spatial Information Sciences*, XXXII (7C2), pp. 132-143.

O' Hara, C., 2005. Managing Dynamic Data. *Earthwide Communications LLC – Earth Imaging Journal*, Vol. March/April, pp. 40-43.

O' Hara, C. 2005: Object- and Feature-Fusion for Multi-Temporal Change Detection and Feature Classification, http://www.definiens-imaging.com/documents/um2005/papers/um2005-ohara.pps (accessed 31 Dec. 2005)

Ricotta, C., Avena, G.C., Volpe, F., 1999. The influence of principal component analysis on the spatial structure of a multispectral dataset. *Int. J. Remote Sensing*, vol. 20, no. 17, pp. 3367-3376.

Sabins, F., 1996. *Remote Sensing: Principles and Interpretation*. W H Freeman & Co., New York.

Zhang, Y., 2002. Problems in the fusion of commercial high resolution satellite as well as Landsat 7 images and initial solutions. In: *The International Archives of the Photogrammetry, Remote Sensing and Spatial Information Sciences*, Vol. XXXIV, part 4, http://studio.gge.unb.ca/UNB/zoomview/Fusion_Zhang_July2002.pdf (accessed 31 Dec. 2005)

Zhang, Y, 2002. A New Automatic Approach for effectively fusing Landsat 7 images and IKONOS images. *IEEE/IGARSS'02*, Toronto, Canada, Jun. 24 - 28, 2002, http://studio.gge.unb.ca/UNB/zoomview/Fusion_poster_2002_50_cUNB.pdf (accessed 31 Dec. 2005)